OXYGEN ISOTOPIC VARIATIONS OF MELILITE CRYSTALS IN A TYPE A CAI FROM ALLENDE.
C. Park[1], S. Wakaki[1], N. Sakamoto[2], S. Kobayashi[2] and H. Yurimoto[1,2], [1]Department of Natural History Sciences, Hokkaido University, Sapporo, 060-0810, Japan (ckpark@ep.sci.hokudai.ac.jp), [2]Isotope Imaging Laboratory, Creative Research Institution Sousei, Hokkaido University, Sapporo, 001-0021, Japan.

Introduction: Ca-Al-rich inclusions (CAIs) in primitive meteorites have been known to be the oldest rocks in the solar system. They firstly formed by condensation from gas, and then may have experienced various thermal processes in the nebula and on the meteorite parent body. Oxygen isotopic compositions of CAI minerals, thus, reflect the solar nebular environments, and may have been disturbed by the alteration and/or thermal metamorphism on the parent body [1, 2].

Melilite is very common mineral in CAIs, which consists of two end members, åkermanite ($Ca_2MgSi_2O_7$) and gehlenite ($Ca_2Al_2SiO_7$) as a solid solution. Especially, reversely zoned melilite is only interpreted as a direct condensate from gas, never molten [3], and oxygen isotopic variations seem to be correlated with chemical zonation [4, 5]. In order to reveal the correlation between oxygen isotopes and chemical composition of a reversely zoned melilite, 2D isotopic imaging is required.

Previous oxygen isotopic study of a Type A inclusion (ON01) from Allende showed that coarse-grained and åkermanite-rich core melilite is uniformly ^{16}O-depleted ($\delta^{18}O$=~0‰), and that the gehlenitic mantle is widely varied from -5 to -45‰ in $\delta^{18}O$ [6]. In addition, mantle is mostly composed of reversely zoned melilite with hibonite, spinel, and perovskite. Anorthite and grossular pseudomorphs are commonly observed as secondary products replacing melilite crystals. Therefore, isotopic imaging for mantle melilite is expected to give insight into mechanism for oxygen isotopic change in the early solar system.

Here we report the 2D isotopic variations of CAI melilites using an isotope-imaging device with secondary ion mass spectrometry [7].

Analytical Methods: A polished thin section of a Type A CAI (ON01) from Allende was studied with energy-dispersive X-ray spectroscopy (EDS) and electron backscatter diffraction (EBSD) system equipped with a field emission gun scanning electron microscope (JEOL JSM-7000F) for mineral chemistry and determination of grain boundaries.

Hokudai isotope microscope system (Cameca ims 1270 + SCAPS imager) was used for oxygen isotope study. A ~1.0 nA Cs^+ primary ion beam was uniformly irradiated onto an elliptical area (~70 μm in traverse diameter) of the sample surface. Negative secondary ions were transmitted through the contrast aperture with 50 μm in diameter in order to obtain high lateral resolution. We set exit slit to 750 μm, and adjusted magnetic field to cut interferences of $^{18}O^-$ peak. A normal incident electron gun was utilized to avoid the electrical charge buildup of analysis area.

Secondary ion images (isotopographs) were acquired for $^{28}Si^-$, $^{27}Al^-$, $^{28}Si^-$, $^{16}O^-$, $^{18}O^-$, and $^{16}O^-$ with accumulated time of 25, 500, 25, 5, 1000, and 5 sec in sequence, respectively. The Si/Al image was adapted to display the chemical zonation of melilite grain. High Si/Al ratio is åkermanite-rich composition. The $^{18}O/^{16}O$ was converted to $\delta^{18}O_{SMOW}$ using $\delta^{18}O$ values from spot analyses conducted before or after isotopography. Image smoothing by moving-average (5x5 kernel) was applied to reduce the statistical error.

Results: Oxygen isotopographs were obtained from reversely zoned melilites (Fig. 1a-d), and alteration phases (e). Statistical error (1σ) of $^{18}O/^{16}O$ in an image is typically 5 to 8‰, and the spatial resolution is ~0.5 μm after image smoothing.

Reversely zoned melilites exhibit a decline of Si/Al ratio from core to rim (Fig. 1a-d). There are three types of oxygen isotope distribution; (1) uniform depletion of ^{16}O ($\delta^{18}O$= -10‰; Fig. 1a), (2) uniform enrichment of ^{16}O ($\delta^{18}O\leq$-40‰; b), (3) oxygen isotopic changes from ^{16}O-poor to ^{16}O-rich, correlated with the reverse zoning, that is, more gehlenitic melilite (low Si/Al) is more ^{16}O-rich ($\delta^{18}O$=-20~-45‰; c, -10~-35‰; d). However, åkermanite contents do not determine the degree of ^{16}O-enrichment.

Oxygen isotopic composition at the grain boundary of two grains is abruptly changed from -10‰ to -25‰ in $\delta^{18}O$ (upper right corner of Fig. 1a). Perovskite adjacent to ^{16}O-poor melilite is -45‰ in $\delta^{18}O$ with a sharp boundary (Fig. 1d-box). Spinel and hibonite grains are always most enriched in ^{16}O ($\delta^{18}O\leq$-45‰).

^{16}O-poor compositions are observed along cracks (Fig. 1b). Alteration phases such as anorthite and grossular pseudomorphs are also homogeneously ^{16}O-depleted ($\delta^{18}O$=~0‰) (Fig. 1e). Oxygen isotopes are gradually changed over boundaries from alteration pseudomorphs to ^{16}O-rich ($\delta^{18}O$=-25‰) melilite.

Discussion: Since reversely zoned melilite can not be explained by crystallization from melts [3], we discuss three possible processes resulting in oxygen isotopic variation of melilite; 1) oxygen isotopic change during crystal growth by condensation, 2) gas-solid diffusion in the nebula, and 3) aqueous alteration and

thermal metamorphism on the parent body. When a solid formed by direct condensation from gas, the isotopic composition of the solid should be same to that of gas. Thus, oxygen isotopes of reversely zoned melilites directly infer the environments of the solar nebula unless they have not been disturbed by 2) and 3).

Recently, [8] suggested that gas-solid diffusion could result in the oxygen isotope change of a Type A CAI at ~1600K. However, our observation showing sharply distinctive $\delta^{18}O$ values along the grain boundary (Fig. 1a) is inconsistent with gas-solid diffusion in the solar nebula. Moreover, if assuming that gas-solid diffusion could result in the oxygen isotopic variation observed in Fig. 1c-d, perovskite adjoining ^{16}O-poor melilite (Fig. 1d-box) should become ^{16}O-poor composition, because oxygen self-diffusion in perovskite [9] is tens of times faster than that in melilite [10] at ~1600K. Thus, we exclude the possibility of gas-solid diffusion in the nebula for the CAI formation.

^{16}O-poor oxygen isotopic compositions are observed along cracks (Fig. 1b) and associated with alteration phases (Fig. 1e), and may diffuse into ^{16}O-rich melilite. These ^{16}O-poor bands are similar to those of [11], possibly due to the fluid-assisted metamorphism [12, 13]. The restricted diffusion area, not universal in the inclusion, can be explained by this hypothesis. However, the wide area of homogeneously ^{16}O-poor composition (Fig. 1a) may not result from the parent body process because of slow oxygen diffusion of melilite and anorthite [10].

Conclusion: With discussion of gas-solid diffusion and fluid-assisted thermal metamorphism, reversely zoned melilites we studied mostly preserve the oxygen isotopic compositions when they formed by condensation from gas. Thus, reversely zoned melilites condensed in the ^{16}O-depleted nebular gas (Fig. 1a) and in the ^{16}O-enriched nebular gas (Fig. 1b), separately. Furthermore, the correlation between oxygen isotopes and chemical zonation (Fig. 1c-d) may indicate that gas composition could change from ^{16}O-poor to ^{16}O-rich during crystal growth by condensation. The melilites may have been disturbed oxygen isotopes in a narrow range by the parent body processes.

References: [1] Yurimoto H. et al. (2008) *Reviews in Mineralogy and Geochemistry,* 68, 141. [2] Krot A.N. et al. (2008) *Geochim. Cosmochim. Acta*, 72, 2534-2555. [3] Macpherson G.J. and Grossman L. (1984) *Geochim. Cosmochim. Acta*, 48, 29-46. [4] Harazono K. and Yurimoto H. (2003) *LPS XXXIV,* Abstract #1540. [5] Katayama J. et al. (2011) abstract in this meeting. [6] Park C. et al. (2010) *Meteoritics & Planet. Sci.,* 73, A5187. [7] Yurimoto H. et al. (2003) *Applied Surface Science*, 203-204, 793-797. [8] Simon J.I. et al. (2011) *Science*, 331, 1175 -1178. [9] Sakaguchi I. and Haneda H. (1996) *Journal of Solid State Chemistry,* 124, 195–197. [10] Ryerson F.J. and McKeegan K.D. (1994) *Geochim. Cosmochim. Acta,* 58, 3713–3734. [11] Nagashima K. et al. (2011) *LPS XXXXII*, Abstract #2509. [12] Wasson J. T. et al. (2001) *Geochim. Cosmochim. Acta*, 65, 4539-4549. [13] Nakamura M. et al. (2005) *Geology*, 33, 829-832.

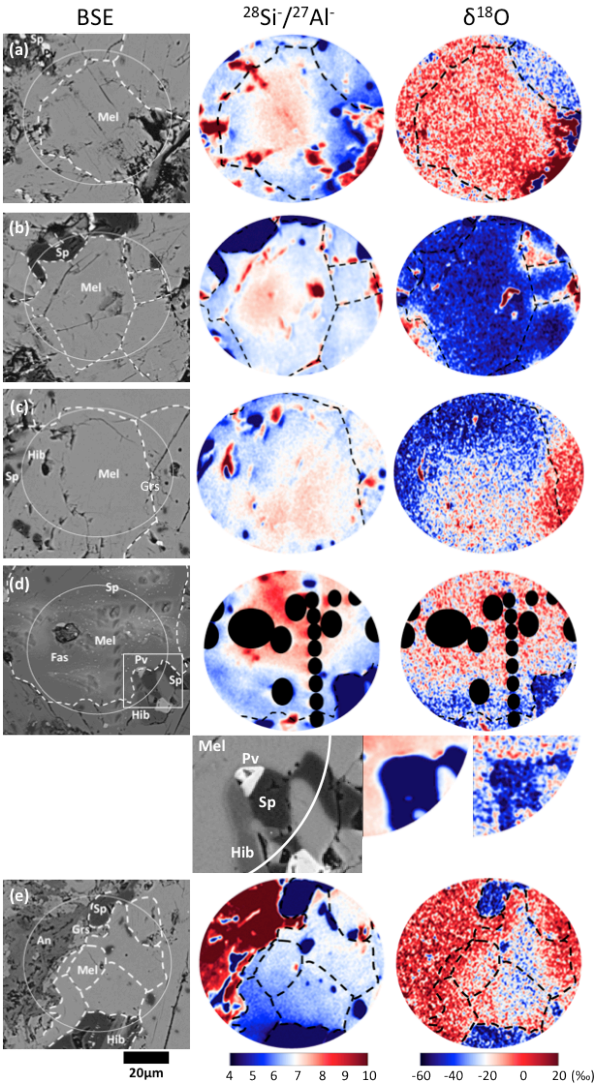

Figure 1. Regions of interest analyzed by SCAPS; (a-d) reversely zoned melilites observed in mantle, and (e) alteration pseudomorphs. Dashed line indicates grain boundaries, and circle on the backscattered-electron (BSE) image marks the analyzed area. Dark filled circles on (d) are previous beam spots and a hole. Scale bar is 20 μm. Mel: melilite, Sp: spinel, Hib: hibonite, Pv: perovksite, Grs: grossular, An: anorthite.